Reconfigurable Directional Lasing Modes in Cavities with Generalized $\mathcal{P}\tilde{\mathcal{T}}$ Symmetry

J. M. Lee,[1] S. Factor,[1] Z. Lin,[1,2] I. Vitebskiy,[3] F. M. Ellis,[1] and T. Kottos[1]
[1]Department of Physics, Wesleyan University, Middletown, Connecticut 06459, USA
[2]School of Engineering and Applied Sciences, Harvard University, Cambridge, Massachusetts 02138, USA
[3]Air Force Research Laboratory, Sensors Directorate, Wright Patterson AFB, Ohio 45433, USA
(Received 20 January 2014; published 25 June 2014)

We introduce a new family of generalized $\mathcal{P}\tilde{\mathcal{T}}$-symmetric cavities that involve gyrotropic elements and support reconfigurable unidirectional lasing modes. We derive conditions for which these modes exist and investigate a simple electronic circuit that experimentally demonstrates their feasibility in the radio-frequency domain.

DOI: 10.1103/PhysRevLett.112.253902 PACS numbers: 42.55.Sa, 05.60.-k, 11.30.Er, 42.25.Bs

In the past few years, there has been great interest in systems that obey parity-time ($\mathcal{PT}$) reversal symmetry [1–20]. In particular, the implementation of $\mathcal{PT}$-symmetric ideas in optics [3–5] and electronics [16–18] has provided experimental grounding of novel $\mathcal{PT}$-symmetric concepts.

At the same time, it has been realized that $\mathcal{PT}$ symmetry is a special case of antilinear operators [14,15,21,22]. Given the success of the former class of systems as hosts of new phenomena, it is natural to expect that extensions to structures that respect other antilinear symmetries might lead to unexpected features and functionalities. Along these lines, it was recently suggested that in contrast to standard linear $\mathcal{PT}$-symmetric systems [2], the interplay of gyrotropic elements with parity-time symmetry allows for nonreciprocal transport [14]. Such structures are invariant under a generalized $\mathcal{P}\tilde{\mathcal{T}}$ symmetry, which incorporates inversion of the gyrotropic element in addition to complex conjugation.

In this paper, we utilize this idea to propose a new class of cavities which can support highly directional reconfigurable lasing modes. The lasing cavity consists of a gyrotropic element sandwiched between two active elements, one with gain and the other one with an equal amount of loss. The total structure is invariant under a generalized $\mathcal{P}\tilde{\mathcal{T}}$ symmetry which enforces new conservation relations for the scattering matrix i.e., $\mathcal{P}\tilde{\mathcal{T}}S\mathcal{P}\tilde{\mathcal{T}} \equiv \mathcal{P}S^{\dagger}\mathcal{P} = S^{-1}$. Under these conditions one can get unidirectional amplification which can turn to lasing at a critical value of the gain and loss parameter. Furthermore, we show that reversing the gain and loss switches the direction of lasing thus achieving a reconfigurable lasing action. We demonstrate the applicability of these ideas in the radio-frequency (rf) domain using a $\mathcal{P}\tilde{\mathcal{T}}$-symmetric RLC circuit. To our knowledge, this is the first experimental demonstration of a system that belongs in the $\mathcal{P}\tilde{\mathcal{T}}$-symmetry class.

For clarity of the presentation we concentrate on one-dimensional scattering setups which allows us to illuminate the basic principles without the unnecessary algebraic complications of higher dimensions. A conceptual visualization of a $\mathcal{P}\tilde{\mathcal{T}}$-symmetric scattering setup is shown in Fig. 1(a). The red area indicates a gain domain (G) while the green a balanced loss (L) element. The cyan area in the middle indicates the existence of a gyrotropic element. A monochromatic wave (with wave vector k) on the right of the scattering domain $V_R = V_R^+ \exp(ikx) + V_R^- \exp(-ikx)$ is related to the wave on the left of the scattering domain $V_L = V_L^+ \exp(ikx) + V_L^- \exp(-ikx)$ via the 2×2 transfer matrix $\mathcal{M}$,

$$\begin{pmatrix} V_R^+ \\ V_R^- \end{pmatrix} = \mathcal{M} \begin{pmatrix} V_L^+ \\ V_L^- \end{pmatrix}. \tag{1}$$

The transmission and reflection coefficients for left (L) and right (R) incident waves can be found using the boundary conditions $V_R^- = 0$ and $V_L^+ = 0$, respectively. These can be expressed in terms of the transfer matrix elements as follows

$$r_L = \frac{-\mathcal{M}_{21}}{\mathcal{M}_{22}}, \qquad t_L = \frac{\det \mathcal{M}}{\mathcal{M}_{22}},$$
$$t_R = \frac{1}{\mathcal{M}_{22}}, \qquad r_R = \frac{\mathcal{M}_{12}}{\mathcal{M}_{22}}. \tag{2}$$

The associated transmittances and reflectances are then defined as $T_{L/R} \equiv |t_{L/R}|^2$ and $R_{L/R} \equiv |r_{L/R}|^2$.

In contrast to unitary scattering processes where $T_L = T_R = T$, $R_L = R_R = R$ and $T + R = 1$ due to flux

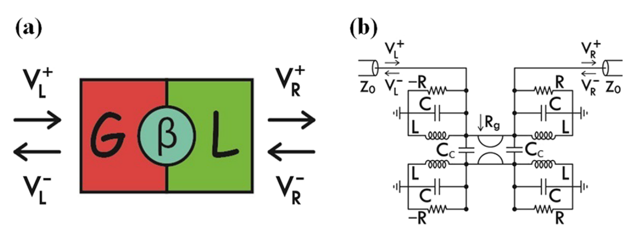

FIG. 1 (color online). (a) A $\mathcal{P}\tilde{\mathcal{T}}$ symmetric cavity. Red indicates gain (G), green indicates loss (L) and β describes the gyrotropic element which is placed symmetrically between the gain and the loss domains. (b) An equivalent $\mathcal{P}\tilde{\mathcal{T}}$- symmetric EC. R_g indicates the gyrator.

conservation, $\mathcal{P}\tilde{\mathcal{T}}$ -symmetric systems satisfy more general conservation relations. To derive them we observe that the parity $\mathcal{P}$ operator interchanges the gain and loss domains of the cavity while at the same time transforms the left (right) incoming (outgoing) amplitudes to their right (left) outgoing (incoming) counterparts, i.e.,

$$\mathcal{P}\begin{pmatrix} V_L^+ \\ V_L^- \end{pmatrix} = \begin{pmatrix} V_R^- \\ V_R^+ \end{pmatrix}, \qquad \mathcal{P}\begin{pmatrix} V_R^+ \\ V_R^- \end{pmatrix} = \begin{pmatrix} V_L^- \\ V_L^+ \end{pmatrix}. \quad (3)$$

The generalized time reversal operator $\tilde{\mathcal{T}}$ maps the incoming (outgoing) wave amplitudes at each side into the outgoing (incoming) ones with a complex conjugation,

$$\tilde{\mathcal{T}}\begin{pmatrix} V_L^+ \\ V_L^- \end{pmatrix} = \begin{pmatrix} V_L^- \\ V_L^+ \end{pmatrix}^*, \qquad \tilde{\mathcal{T}}\begin{pmatrix} V_R^+ \\ V_R^- \end{pmatrix} = \begin{pmatrix} V_R^- \\ V_R^+ \end{pmatrix}^*. \quad (4)$$

In addition, the $\tilde{\mathcal{T}}$ operator interchanges the gain and loss elements in the cavity and reverses the direction of the gyrotropy $\beta \to -\beta$. Combining the action of the $\mathcal{P}$ and $\tilde{\mathcal{T}}$ operators we get

$$\begin{pmatrix} V_L^+ \\ V_L^- \end{pmatrix}^* = \mathcal{M}(-\beta)\begin{pmatrix} V_R^+ \\ V_R^- \end{pmatrix}^*, \quad (5)$$

which together with Eq. (1) leads to the relation [14]

$$\mathcal{M}^*(-\beta)\mathcal{M}(\beta) = 1 \to \begin{pmatrix} 0 & 1 \\ -1 & 0 \end{pmatrix}\mathcal{M}^\dagger\begin{pmatrix} 0 & -1 \\ 1 & 0 \end{pmatrix} = \mathcal{M}. \quad (6)$$

The second equation in (6) results from the first one after employing the relation $\mathcal{M}(-\beta) = [1/\det\mathcal{M}(\beta)]\mathcal{M}(\beta)$ imposed by the symmetry of the gyrotropic element [23]. It is straightforward to show that Eq. (6) leads to the following relations [15]:

$$\mathrm{Re}[t_L r_R^*] = 0, \quad \mathrm{Re}[t_R r_L^*] = 0, \quad t_L t_R^* + r_R r_L^* = 1. \quad (7)$$

We stress that, in contrast to standard $\mathcal{PT}$ symmetric systems where $t_L = t_R$, here the left and right transmissions are not necessarily equal to one another leading to a nonreciprocal transport [14].

Equations (7) are the consequences of generalized unitary relations satisfied by the scattering matrix S [14,15]. The latter provides an alternative formulation of the scattering process in terms of incoming and outgoing waves:

$$\begin{pmatrix} V_L^- \\ V_R^+ \end{pmatrix} = \mathcal{S}\begin{pmatrix} V_L^+ \\ V_R^- \end{pmatrix}, \qquad S = \begin{pmatrix} r_L & t_R \\ t_L & r_R \end{pmatrix}. \quad (8)$$

Using Eq. (2) together with Eq. (6), we get the following equivalent relations for the scattering matrix:

$$\mathcal{P}\tilde{\mathcal{T}}\mathcal{S}\mathcal{P}\tilde{\mathcal{T}} = \mathcal{S}^{-1}; \quad \mathcal{S}\mathcal{P}\mathcal{S}^\dagger\mathcal{P} = 1, \quad \mathcal{P} = \begin{pmatrix} 0 & 1 \\ 1 & 0 \end{pmatrix}. \quad (9)$$

The eigenvalues of the $\mathcal{P}\tilde{\mathcal{T}}$-symmetric $\mathcal{S}(\beta)$ matrices are not necessarily unimodular. To demonstrate this property, we consider an eigenvector $\hat{v}_n$ of the $\mathcal{S}(\beta)$ matrix with associated eigenvalue $s_n(\beta)$. Using Eq. (9) we get

$$\mathcal{S}(\beta)\mathcal{P}\tilde{\mathcal{T}}\hat{v}_n(\beta) = \mathcal{P}\tilde{\mathcal{T}}\mathcal{S}^{-1}(\beta)\hat{v}_n(\beta) = \frac{1}{s_n^*(-\beta)}\mathcal{P}\tilde{\mathcal{T}}\hat{v}_n(\beta), \quad (10)$$

where for the last equality we have used the fact that the eigenvalues of $\mathcal{S}^{-1}(\beta)$ are $1/s_n(\beta)$ and that the action of $\tilde{\mathcal{T}}$ on them is $\tilde{\mathcal{T}}(1/s_n(\beta)) = 1/s_n^*(-\beta)$. Equation (10) indicates that $\mathcal{P}\tilde{\mathcal{T}}\hat{v}_n$ is also an eigenvector of $\mathcal{S}$ with eigenvalue $1/s_n^*(-\beta)$. We distinguish between two scenarios: In the first case, the scattering matrix S and the $\mathcal{P}\tilde{\mathcal{T}}$ operator share the same eigenvector $\hat{v}_n$. Then Eq. (10) leads to $s_n(\beta)\hat{v}_n = [1/(s_n^*(-\beta))]\hat{v}_n$. In this case we find that the eigenvalues satisfy the relation $s_n(\beta)s_n^*(-\beta) = 1$ and the corresponding eigenstates $\hat{v}_n$ exhibit no net amplification or attenuation; the system is in the *exact phase*. The alternative scenario involves the case where $\hat{v}_n$ itself is not $\mathcal{P}\tilde{\mathcal{T}}$-symmetric. In this case the pair of eigenvectors of the $\mathcal{S}$ matrix can be transformed to one another via the $\mathcal{P}\tilde{\mathcal{T}}$ operator i.e., $\mathcal{P}\tilde{\mathcal{T}}\hat{v}_n = \hat{v}_m$. The corresponding eigenvalues satisfy the relation $s_m(\beta)s_n^*(-\beta) = 1$, with one eigenvector exhibiting amplification and the other attenuation; the system is in the *broken phase*.

The boundary between the exact and broken phases can be found directly by analysis of the eigenvalues of the scattering matrix $\mathcal{S}$. The latter can be parametrized in terms of four numbers $\mathrm{Re}(a); \mathrm{Im}(a); b; c$ $(b, c \in \mathcal{R})$ as

$$S = \frac{1}{a}\begin{pmatrix} ic & 1 \\ |a|^2 - bc & ib \end{pmatrix}. \quad (11)$$

The corresponding eigenvalues are $\frac{1}{2a}[i(b+c) \pm \sqrt{4|a|^2 - (b+c)^2}]$ and they are unimodular (exact phase) when $4|a|^2 - (b+c)^2 \geq 0$. The equality is satisfied at the spontaneous $\mathcal{P}\tilde{\mathcal{T}}$-symmetric phase transition. The latter condition can be written in terms of r_L, r_R as

$$|r_L|^2 + |r_R|^2 + 2r_L r_R^* = 4. \quad (12)$$

Next, we define the conditions at which a $\mathcal{P}\tilde{\mathcal{T}}$-symmetric system behaves as a unidirectional laser. We require that the output field in one direction, say the left, be amplified while attenuated in the opposite direction. In terms of transmissions and reflections, the above condition reads as

$$r_L \to \infty; \qquad t_L \to 0; \qquad t_R \to \infty; \qquad r_R \to 0. \quad (13)$$

Equations (13) and the $\mathcal{P}\tilde{\mathcal{T}}$-symmetric constrains Eqs. (7) can be simultaneously satisfied. Equations (13) are written in terms of $\mathcal{M}$-matrix elements using Eq. (2). We get

$$\begin{aligned} &\mathcal{M}_{22}(\omega,\beta,\gamma)=0 \qquad \text{(lasing condition)} \\ &\mathcal{M}_{12}(\omega,\beta,\gamma)=0 \qquad \text{(unidirectionality condition)}. \end{aligned} \tag{14}$$

In this framework, the complex frequencies ω for which $\mathcal{M}_{22}(\omega,\beta,\gamma)=0$, correspond to the poles of the scattering matrix. Due to flux conservation and causality relations they lie on the lower part of the complex plane when a parameter γ that controls the degree of gain and loss strength of the two active elements is equal to zero. As γ is increased, the poles move towards the real axis. Lasing action is achieved at a critical $\gamma_{\rm cr}$, at which the first of these poles $\omega_{\rm cr}$ crosses the real axis. If the second condition in Eq. (14) is also satisfied at $\omega_{\rm cr}$, we get $\det\mathcal{M}\to 0\neq 1$ which characterizes nonreciprocal transport in $\mathcal{P}\tilde{\mathcal{T}}$-symmetric systems (see Eqs. (2) and [14]).

The direction of the unidirectional lasing mode can be reversed (say from left to right) by interchanging the spatial distribution of gain and loss elements i.e., $\gamma\to-\gamma$. Application of the parity operator Eq. (3) to the transfer matrix relation Eq. (1) results in the relation

$$\begin{pmatrix} V_L^- \\ V_L^+ \end{pmatrix} = \mathcal{M}(-\gamma)\begin{pmatrix} V_R^- \\ V_R^+ \end{pmatrix}. \tag{15}$$

Using Eq. (15), together with the boundary condition $V_R^-=0$ we get that $V_L^-/V_L^+=M_{12}(-\gamma)/M_{22}(-\gamma)$ and $V_R^+/V_L^+=1/M_{22}(-\gamma)$. The left sides of these equalities (supplemented with the boundary condition $V_R^-=0$) define $r_L(\gamma)$ and $t_L(\gamma)$ respectively. The right sides are equal to $r_R(-\gamma)$ and $t_R(-\gamma)$ [see the definitions Eqs. (2)]. Therefore, $r_L(\gamma)=r_R(-\gamma)$ and $t_L(\gamma)=t_R(-\gamma)$ which allows us to conclude that reversing the gain and loss in a unidirectional lasing cavity that supports, say left lasing action [satisfying Eq. (13)], will result in a right unidirectional lasing.

We demonstrate the validity of the $\mathcal{P}\tilde{\mathcal{T}}$-symmetric unidirectional lasing utilizing the framework of electronic circuits. Our system [see Fig. 1(b)] consists of two pairs of capacitively coupled RLC oscillators, one with amplification [left side of Fig. 1(b)] and the other with equivalent attenuation [right side of Fig. 1(b)]. The loss is provided by standard resistors R while gain is implemented with a negative impedance converter (NIC) $-R$. The gain and loss parameter is defined as $\gamma=\sqrt{L/C}/R$, the uncoupled frequency of each resonator is $\omega_0=1/\sqrt{LC}$, and the capacitive coupling between the two pairs is $C_c=\kappa C$. The circuit is connected to transmission lines (TL) with impedance Z_0 on each side. We also define a dimensionless TL conductance $\eta=\sqrt{L/C}/Z_0$.

The gyrotropic element that it is responsible for the violation of standard time-reversal symmetry (i.e., $t\to-t$) is implemented in the circuit via a gyrator [(center of Fig. 1(b)]. This is a lossless two-port network component which connects the input and output voltages $\mathbf{V}\equiv(V_n,V_m)^T$ and currents $\mathbf{I}\equiv(I_n,I_m)^T$ associated with ports n and m as

$$\begin{pmatrix} V_n \\ V_m \end{pmatrix} = \begin{pmatrix} 0 & -R_g \\ R_g & 0 \end{pmatrix}\begin{pmatrix} I_n \\ I_m \end{pmatrix}; \quad R_g=\beta^{-1}\sqrt{\frac{L}{C}}, \tag{16}$$

where β is a dimensionless conductance. Equation (16) is invariant under a generalized time reversal operator $\tilde{\mathcal{T}}$ which performs time-inversion ($t\to-t$) together with the transformation $\beta\to-\beta$.

In the TL the wave can be decomposed into forward and backward components with corresponding amplitudes $V_{L/R}^+$ and $V_{L/R}^-$, respectively. Matching boundary conditions at the TL-EC contact requires that

$$V_{L/R}=V_{L/R}^+ + V_{L/R}^-; I_{L/R}=[V_{L/R}^+ - V_{L/R}^-]/Z_0, \tag{17}$$

where $V_{L/R}$ and $I_{L/R}$ are the voltages and currents at the left (L) and right (R) contacts. Equations (17) assume incoming current from the left TL and outgoing current into the right TL. The associated reflections or transmissions are $r_{L/R}\equiv V_{L/R}^{\mp}/V_{L/R}^{\pm}$ and $t_{L/R}\equiv V_{R/L}^{\pm}/V_{L/R}^{\pm}$ [see Eqs. (2)].

Application of circuit laws at the TL-EC contacts yields the following expressions for the current and voltage amplitudes:

$$\begin{aligned} &i[\gamma V_L-\beta(V_1-V_2)]-\omega[V_L+\kappa(V_L-V_1)]+\frac{V_L}{\omega}=-i\eta Z_0 I_L \\ &i[\gamma V_R-\beta(V_1-V_2)]+\omega[V_R+\kappa(V_R-V_2)]-\frac{V_R}{\omega}=-i\eta Z_0 I_R \\ &i[\gamma V_1-\beta(V_L-V_R)]-\omega[V_1-\kappa(V_L-V_1)]+\frac{V_1}{\omega}=0 \\ &i[\gamma V_2-\beta(V_L-V_R)]+\omega[V_2-\kappa(V_R-V_2)]-\frac{V_2}{\omega}=0, \end{aligned} \tag{18}$$

where ω is a dimensionless frequency in units of ω_0. Note that Eqs. (18) are invariant under combined $\mathcal{P}$ ($L\leftrightarrow R$, $1\leftrightarrow 2$) and $\tilde{\mathcal{T}}$ ($i\leftrightarrow -i$, $\beta\leftrightarrow-\beta$) reversal. The resulting $\mathcal{M}$ matrix takes the form

$$\mathcal{M}=\begin{pmatrix} (a+ib) & i(c-d) \\ i(c+d) & (a-ib) \end{pmatrix}/A, \tag{19}$$

where a,b,c,d,A are polynomials in ω and their exact form is given in the Supplemental Material [24]. One can check that the $\mathcal{M}$ matrix satisfies Eq. (6).

As discussed previously, the condition $\det\mathcal{M}\to 0$ is a necessary (but not sufficient) condition for unidirectional lasing. Assuming constant coupling κ, we get

$$\begin{aligned} \det\mathcal{M} &= \frac{\beta(1-\omega^2(1+\kappa))-\gamma\kappa\omega^2}{\beta(1-\omega^2(1+\kappa))+\gamma\kappa\omega^2} \\ &= 0 \to \beta=\frac{\gamma\kappa\omega^2}{1-\omega^2(1+\kappa)}. \end{aligned} \tag{20}$$

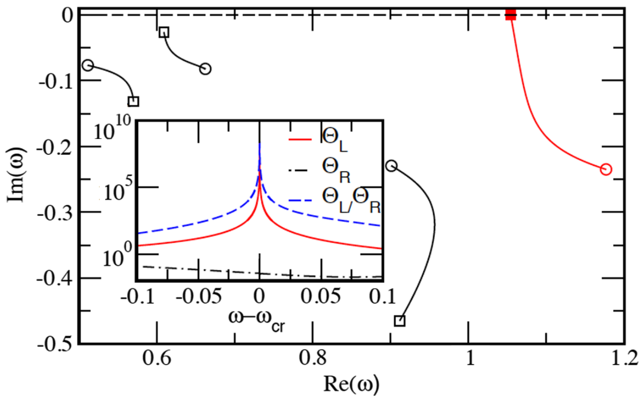

FIG. 2 (color online). Evolution of resonances ω vs γ. The value of the gyrotropic element β is fixed to be $\beta = \beta_{\rm cr} = -0.50609$ and the capacitive coupling is $\kappa = 0.8$. The dimensionless TL conductance is $\eta = 0.9$. The unidirectional lasing frequency (red square) is $\omega_{\rm cr} = 1.05394$ and it occurs at $\gamma_{\rm cr} = 0.56919$. Inset: The overall left and right outgoing coefficient $\Theta_{L/R}$. A divergence of Θ_L at $\omega_{\rm cr}$ indicates a left unidirectional lasing action. In the same inset we also report the ratio Θ_L/Θ_R.

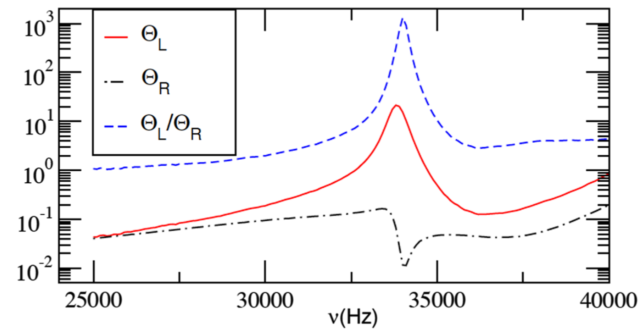

FIG. 3 (color online). Experimental results for the overall left or right outgoing coefficient $\Theta_{L/R}$. A divergence of Θ_L at $\omega_{\rm cr}$ indicates a left unidirectional lasing action. In the same figure we also report the ratio Θ_L/Θ_R. The parameters used in the experiment are $L = 1.4\ \mu$H, $C = 10$ nF, $C_c = 3$ nF, $R = 2.7$ kΩ, $Z_0 = 1.35$ kΩ, and $Rg = 4.7$ kΩ.

Next we find the set of $\omega_{\rm cr}, \gamma_{\rm cr}, \beta_{\rm cr}$, values for which $\mathcal{M}_{22}(\gamma_{\rm cr}, \beta_{\rm cr}, \omega_{\rm cr}) = 0$ and $\mathcal{M}_{12}(\gamma_{\rm cr}, \beta_{\rm cr}, \omega_{\rm cr}) = 0$ are simultaneously satisfied. The latter is achieved by substituting Eq. (20) in these two relations. In Fig. 2 we plot the evolution of complex zeros of $\mathcal{M}_{22}(\omega, \gamma; \beta = \beta_{\rm cr})$ as the gain and loss parameter γ increases and for a fixed value of the magnetic field $\beta_{\rm cr}$. At a critical value $\gamma = \gamma_{\rm cr}$ the first resonance crosses the real axes at $\omega = \omega_{\rm cr}$ and a unidirectional lasing is achieved.

We confirm the existence of a unidirectional lasing mode by introducing an overall left or right outgoing coefficient $\Theta_{L/R}(\omega, \gamma, \beta)$, defined as the ratio of the left or right outgoing field intensity to the total incident intensity:

$$\Theta_L = \frac{|V_L^-|^2}{|V_L^+|^2 + |V_R^-|^2}; \qquad \Theta_R = \frac{|V_R^+|^2}{|V_L^+|^2 + |V_R^-|^2}. \tag{21}$$

Whenever $\Theta_L \gg 1$ ($\Theta_R \gg 1$) while $\Theta_R \approx 0$ ($\Theta_L \approx 0$) a left (right) unidirectional laser has been achieved. At $\omega = \omega_{\rm cr}$, the outgoing coefficient $\Theta(\omega_{\rm cr})$ diverges, i.e., $\Theta_L \to \infty$ ($\Theta_R \to \infty$), signalling the transition to left (right) lasing action. Typical behavior of $\Theta_{L/R}$ near a left unidirectional lasing mode (associated with the parameter values of Fig. 2(a)] is shown in the inset of Fig. 2. We see that around $\omega = \omega_{\rm cr}$, the Θ_L is very large while it diverges at $\omega = \omega_{\rm cr}$. At the same time, Θ_R acquires a small constant value $\mathcal{O}(10^{-2})$ around $\omega_{\rm cr}$ while it becomes zero at $\omega = \omega_{\rm cr}$.

The demonstration of these principles in the context of electronics requires the implementation of the electronic gyrator of Fig. 1(b), defined by Eq. (16). We point out that the possibility of an ideal, passive, four-terminal gyrator in the Kirchoff limit of electronics has not yet been realized. Recent developments in magnetoelectric devices based on laminates of magnetostrictive and piezoelectric materials [25] have demonstrated promising gyrotropic coupling. For these reasons, along with a clean comparison to the ideas presented in this work, we implement a near-ideal gyrator using active components discussed in detail in the Supplemental Material [24].

Figure 3 shows experimental results for the left and right outgoing coefficients $\Theta_{L/R}(\omega, \gamma, \beta)$ of Eq. (21) for a circuit based on four LRC resonators. The two negative resistances are based on positive feedback with $LM356$ op-amps [16]. Experimentally, the values used (see caption of Fig. 3) were based primarily on the limitations of the op-amps used for the gyrator and negative resistances, with the exact transmission line impedance carefully adjusted to just below the circuit instability (lasing) threshold. Under this condition, scattering parameters used for $\Theta_{L/R}(\omega)$ were deduced from circuit voltages captured by a four-channel oscilloscope. The corresponding scaled parameters for the data shown were $\gamma = 0.23875$, $\beta = 0.765$, $\kappa = 0.356$, and $\eta = 0.38$. Above threshold, the circuit exhibits self-oscillatory exponential growth of the single linear mode at ω_{cr}, ultimately leading to complex saturation dynamics beyond the scope of this investigation.

The proximity in parameter space to a system instability threshold is responsible for two near-threshold modes corresponding to those in Fig. 2 imposed by the $\mathcal{P}\tilde{\mathcal{T}}$ symmetry. Figure 3 shows the left unidirectional mode associated with the experimental parameters used. The asymmetric phase inversion that characterizes the gyrator transmission combined with the coupled oscillator phases is ultimately responsible for the expression of asymmetry in the left and right mode amplitudes shown.

We have shown that $\mathcal{P}\tilde{\mathcal{T}}$-symmetric structures combined with gyrotropic components are capable of directionally controlled power output. Furthermore we show that reversing the gain and loss results in reconfiguring the lasing action. An experimental demonstration of the phenomenon in an electronic circuit illustrates the physics, emphasizing the crucial role of phase-reversed coupling provided by the gyrator. It will be interesting to implement these ideas in the optics framework using, for example, $\mathcal{P}\tilde{\mathcal{T}}$-symmetric structures like the ones discussed in Ref. [14]. Potential applications of such $\mathcal{P}\tilde{\mathcal{T}}$-symmetric lasers include optical ring gyroscopes in which a beat frequency between two oppositely directed $\mathcal{P}\tilde{\mathcal{T}}$ lasers is detected to measure the rotation rate, optical logic elements in which the direction of lasing in a ring is the logic state of the device, etc.

This work is partly sponsored by the Air Force Research Laboratory (AFRL/RYDP) through the AMMTIAC contract with Alion Science and Technology and partly by the Air Force Office of Scientific Research LRIR09RY04COR and FA 9550-10-1-0433, AFOSR MURI Grant No. FA9550-14-1-0037, and an NSF Grant No. ECCS-1128571.

[1] C. M. Bender and S. Boettcher, Phys. Rev. Lett. **80**, 5243 (1998); C. M. Bender, Rep. Prog. Phys. **70**, 947 (2007).

[2] K. G. Makris, R. El-Ganainy, D. N. Christodoulides, and Z. H. Musslimani, Phys. Rev. Lett. **100**, 103904 (2008).

[3] C. E. Rüter, K. G. Makris, R. El-Ganainy, D. N. Christodoulides, M. Segev, and D. Kip, Nat. Phys. **6**, 192 (2010); A. Guo, G. J. Salamo, D. Duchesne, R. Morandotti, M. Volatier-Ravat, V. Aimez, G. A. Siviloglou, and D. N. Christodoulides, Phys. Rev. Lett. **103**, 093902 (2009).

[4] A. Regensburger, C. Bersch, M.-A. Miri, G. Onishchukov, D. N. Christodoulides, and Ulf Peschel, Nature (London) **488**, 167 (2012).

[5] L. Feng, Y.-L. Xu, W. S. Fegadolli, M.-H. Lu, J. E. B. Oliveira, V. R. Almeida, Y.-F. Chen, and A. Scherer, Nat. Mater. **12**, 108 (2013).

[6] A. Mostafazadeh, Phys. Rev. Lett. **102**, 220402 (2009).

[7] S. Longhi, Phys. Rev. Lett. **103**, 123601 (2009); S. Longhi, Phys. Rev. Lett. **105**, 013903 (2010).

[8] M. C. Zheng, D. N. Christodoulides, R. Fleischmann, and T. Kottos, Phys. Rev. A **82**, 010103 (2010).

[9] H. Schomerus, Phys. Rev. Lett. **104**, 233601 (2010).

[10] A. A. Sukhorukov, Z. Xu, and Y. S. Kivshar, Phys. Rev. A **82**, 043818 (2010).

[11] S. Longhi, Phys. Rev. A **82**, 031801 (2010); Y. D. Chong, L. Ge, and A. D. Stone, Phys. Rev. Lett. **106**, 093902 (2011).

[12] H. Ramezani, D. N. Christodoulides, V. Kovanis, I. Vitebskiy, and T. Kottos, Phys. Rev. Lett. **109**, 033902 (2012); H. Ramezani, T. Kottos, V. Kovanis, and D. N. Christodoulides, Phys. Rev. A **85**, 013818 (2012).

[13] N. Lazarides and G. P. Tsironis, Phys. Rev. Lett. **110**, 053901 (2013); D. Wang and A. B. Aceves, Phys. Rev. A **88**, 043831 (2013).

[14] H. Ramezani, Z. Lin, S. Kalish, T. Kottos, V. Kovanis, and I. Vitebskiy, Opt. Express **20**, 26200 (2012); J. M. Lee, Z. Lin, H. Ramezani, F. M. Ellis, V. Kovanis, I. Vitebskiy, and T. Kottos, arXiv:1303.0774.

[15] H. Schomerus, Phil. Trans. R. Soc. A **371**, 20120194 (2013).

[16] J. Schindler, Z. Lin, J. M. Lee, H. Ramezani, F. M. Ellis, and T. Kottos, J. Phys. A: Math. Theor. **45**, 444029 (2012); H. Ramezani, J. Schindler, F. M. Ellis, U. Gunther, and T. Kottos, Phys. Rev. A **85**, 062122 (2012); Z. Lin, J. Schindler, F. M. Ellis, and T. Kottos, Phys. Rev. A **85**, 050101(R) (2012).

[17] J. Cuevas, P. G. Kevrekidis, A. Saxena, and A. Khare, Phys. Rev. A **88**, 032108 (2013).

[18] N. Bender, S. Factor, J. D. Bodyfelt, H. Ramezani, D. N. Christodoulides, F. M. Ellis, and T. Kottos, Phys. Rev. Lett. **110**, 234101 (2013).

[19] C. T. West, T. Kottos, and T. Prosen, Phys. Rev. Lett. **104**, 054102 (2010); C. Birchall and H. Schomerus, J. Phys. A **45**, 444006 (2012).

[20] E.-M. Graefe, J. Phys. A **45**, 444015 (2012); M. Hiller, T. Kottos, and A. Ossipov, Phys. Rev. A **73**, 063625 (2006); M. K. Oberthaler, R. Abfalterer, S. Bernet, J. Schmiedmayer, and A. Zeilinger, Phys. Rev. Lett. **77**, 4980 (1996).

[21] A. Mostafazadeh, J. Math. Phys. (N.Y.) **43**, 205 (2002); A. MostafazadehJ. Math. Phys. (N.Y.)**43**, 3944 (2002); A. Mostafazadeh, J. Phys. A **41**, 055304 (2008).

[22] C. M. Bender, M. V. Berry, A. Mandilara, J. Phys. A **35**, L467 (2002).

[23] A gyrotropic scattering unit has a scattering matrix S_g which satisfies the fundamental symmetry relation $S_g(-\beta) = S_g^T(\beta)$ [26]. Based on the relation between impedance and scattering matrices $S_g \equiv ((Z_0 - Z_g)/(Z_0 + Z_g))$ (Z_0 is the characteristic impedance of the ports) one can also show that $Z_g(-\beta) = Z_g^T(\beta)$. Using the relation between the scattering matrix elements and transfer matrix elements [see Eq. (2)] we can show that $\mathcal{M}_g(-\beta) = [1/\det \mathcal{M}_g(\beta)]\mathcal{M}_g(\beta)$. Furthermore, for a cavity or system consisting of various units [see Fig. 1(a) where there are three scattering units: Left (gain)/center (gyrotropic)/Right (loss)] the total transfer matrix $\mathcal{M}$ is the product of individual transfer matrices and thus $\mathcal{M}(-\beta) = \mathcal{M}_L \times \mathcal{M}_g(-\beta) \times \mathcal{M}_R = [1/\det \mathcal{M}(\beta)]\mathcal{M}(\beta)$. Here it is assumed that $\det[\mathcal{M}_L] = \det[\mathcal{M}_R] = 1$.

[24] See Supplemental Material at http://link.aps.org/supplemental/10.1103/PhysRevLett.112.253902 for (a) exact expressions of the transfer matrix elements and (b) a discussion of gyrator implementation.

[25] M. Li, D. Hasanyan, Y. Wang, J. Gao, J. Li, and D. Viehland, J. Phys. D **45**, 355002 (2012).

[26] P. A. Mello and N. Kumar, *Quantum Transport in Mesoscopic Systems: Complexity and Statistical Fluctuations : A Maximum-Entropy Viewpoint*, Volume 4, Mesoscopic Physics and Nanotechnology (Oxford University Press, New York, 2004).